

TIMING OF FIVE MILLISECOND PULSARS DISCOVERED IN THE PALFA SURVEY

P. SCHOLZ¹, V. M. KASPI¹, A. G. LYNE², B. W. STAPPERS², S. BOGDANOV³, J. M. CORDES⁴, F. CRAWFORD⁵, R. D. FERDMAN¹, P. C. C. FREIRE⁶, J. W. T. HESSELS^{7,8}, D. R. LORIMER⁹, I. H. STAIRS¹⁰, B. ALLEN^{11,12,13}, A. BRAZIER^{4,14}, F. CAMILO³, R. F. CARDOSO⁹, S. CHATTERJEE⁴, J. S. DENEVA¹⁵, F. A. JENET¹⁶, C. KARAKO-ARGAMAN¹, B. KNISPEL^{12,13}, P. LAZARUS⁶, K. J. LEE⁶, J. VAN LEEUWEN^{7,8}, R. LYNCH¹, E. C. MADSEN¹, M. A. McLAUGHLIN⁹, S. M. RANSOM¹⁷, X. SIEMENS¹¹, L. G. SPITLER⁶, K. STOVALL¹⁸, J. K. SWIGGUM⁹, A. VENKATARAMAN¹⁹, AND W. W. ZHU¹⁰

Draft version March 1, 2024

ABSTRACT

We present the discovery of five millisecond pulsars (MSPs) from the PALFA Galactic plane survey using Arecibo. Four of these (PSRs J0557+1551, J1850+0244, J1902+0300, and J1943+2210) are binary pulsars whose companions are likely white dwarfs, and one (PSR J1905+0453) is isolated. Phase-coherent timing solutions, ranging from ~ 1 to ~ 3 years in length, and based on observations from the Jodrell Bank and Arecibo telescopes, provide precise determinations of spin, orbital, and astrometric parameters. All five pulsars have large dispersion measures ($> 100 \text{ pc cm}^{-3}$, within the top 20% of all known Galactic field MSPs) and are faint (1.4 GHz flux density $\lesssim 0.1 \text{ mJy}$, within the faintest 5% of all known Galactic field MSPs), illustrating PALFA's ability to find increasingly faint, distant MSPs in the Galactic plane. In particular, PSR J1850+0244 has a dispersion measure of 540 pc cm^{-3} , the highest of all known MSPs. Such distant, faint MSPs are important input for accurately modeling the total Galactic MSP population.

Keywords: pulsars: general — pulsars: individual (PSR J0557+1551, PSR J1850+0244, PSR J1902+0300, PSR J1905+0453, PSR J1943+2210)

1. INTRODUCTION

Millisecond pulsars (MSPs) are neutron stars that have been spun up by accretion to extremely fast spin periods ($P < 20 \text{ ms}$) (Alpar et al. 1982; Radhakrishnan & Srinivasan 1982). The first discovered

MSP, PSR B1937+21, was found in 1982 (Backer et al. 1982) and since then ~ 160 Galactic MSPs have been discovered (~ 130 MSPs have been found in globular clusters) in different pulsar surveys (for a review of past and ongoing searches for MSPs see Stovall et al. 2013). MSPs are of great scientific value, giving us insight into many different branches of fundamental physics and astrophysics, as we elaborate below.

Most MSPs are found in binary systems with a low-mass, degenerate companion. These companions are responsible for spinning-up such pulsars to millisecond rotational periods by transferring mass and angular momentum onto them. The discovery of new MSP binaries can test (and in some cases confirm) models of binary evolution (e.g. Phinney & Kulkarni 1994; Tauris & Savonije 1999; Archibald et al. 2009; Papitto et al. 2013) and sometimes challenge them, as in the case of PSR J1903+0327 (Champion et al. 2008), which suggested that formation in a triple stellar system occurs in some cases (Freire et al. 2011; Portegies Zwart et al. 2011). This was also directly demonstrated in the recently discovered PSR J0337+1715 triple system (Ransom et al. 2014). On the other hand, isolated MSPs exist as well, and their origin is an important open question (Bailyn & Grindlay 1990; Levinson & Eichler 1991; Bailes et al. 2011).

The continued discovery of MSPs is also motivated by their potential for aiding the detection of gravitational waves. High-precision, long-term timing of MSPs forming a ‘pulsar timing array’ (Foster & Backer 1990) could allow the detection of gravitational waves in the nanohertz frequency range particularly in the form of a stochastic background that is due to super-massive black-hole mergers at high redshifts (van Haasteren et al. 2011; Yardley et al. 2011; Demorest et al. 2013; Shannon et al. 2013). The discovery of more MSPs that can be

¹ Department of Physics, McGill University, Montreal, QC H3A 2T8, Canada; pscholz@physics.mcgill.ca

² Jodrell Bank Centre for Astrophysics, School of Physics and Astronomy, University of Manchester, Manchester, M13 9PL, UK

³ Columbia Astrophysics Laboratory, Columbia University, New York, NY 10027, USA

⁴ Department of Astronomy, Cornell University, Ithaca, NY 14853, USA

⁵ Department of Physics and Astronomy, Franklin and Marshall College, Lancaster, PA 17604-3003, USA

⁶ Max-Planck-Institut für Radioastronomie, D-53121 Bonn, Germany

⁷ ASTRON, Netherlands Institute for Radio Astronomy, Postbus 2, 7990 AA, Dwingeloo, The Netherlands

⁸ Anton Pannekoek Institute for Astronomy, University of Amsterdam, Science Park 904, 1098 XH, Amsterdam, The Netherlands

⁹ Department of Physics and Astronomy, West Virginia University, Morgantown, WV 26506, USA

¹⁰ Department of Physics and Astronomy, University of British Columbia, 6224 Agricultural Road Vancouver, BC V6T 1Z1, Canada

¹¹ Physics Department, University of Wisconsin-Milwaukee, Milwaukee WI 53211, USA

¹² Leibniz Universität Hannover, D-30167 Hannover, Germany

¹³ Max-Planck-Institut für Gravitationsphysik, D-30167 Hannover, Germany

¹⁴ Cornell Center for Advanced Computing, Cornell University, Ithaca, NY 14853, USA

¹⁵ Naval Research Laboratory, 4555 Overlook Ave SW, Washington, DC 20375, USA

¹⁶ Center for Gravitational Wave Astronomy, University of Texas at Brownsville, TX 78520, USA

¹⁷ NRAO, Charlottesville, VA 22903, USA

¹⁸ Department of Physics and Astronomy, University of New Mexico, NM, 87131, USA

¹⁹ Arecibo Observatory, HC3 Box 53995, Arecibo, PR 00612, USA

timed with very high precision is crucial for this effort to succeed. Some MSP binaries also enable tests of General Relativity and alternate theories of relativistic gravity (e.g. Gonzalez et al. 2011; Freire et al. 2012; Antoniadis et al. 2013) as well as measure precise component masses that can test models of neutron-star interiors (e.g. Demorest et al. 2010; Lattimer & Prakash 2010; Bednarek et al. 2012).

PALFA is a pulsar survey using the 7-beam Arecibo L-Band Feed Array (ALFA) on the Arecibo Observatory William E. Gordon 305-m Telescope. The survey’s centre frequency is 1.4 GHz, and the planned survey coverage is the region of the Galactic plane ($|b| < 5^\circ$) accessible from the Arecibo telescope ($32^\circ \lesssim l \lesssim 77^\circ$ and $168^\circ \lesssim l \lesssim 214^\circ$). The survey began in 2004 and is ongoing (Cordes et al. 2006; Lazarus 2013).

PALFA provides a unique window for the discovery of MSPs. Its high sensitivity allows observations with short integration times which mitigate the effects of Doppler smearing of the pulsed signal in the case of a tight binary orbit (Johnston & Kulkarni 1991). The increased sensitivity and relatively high observing frequency – which reduces the deleterious effects of dispersion-smearing and multi-path scattering – compared to other surveys also allow PALFA to find MSPs at much further distances and higher dispersion measures (DMs). Figure 1 shows the unique parameter space probed by PALFA.

The discovery of distant, highly dispersed MSPs will allow a more complete characterization of the Galactic MSP population. Current models of the Galactic MSP population are based primarily on the Parkes Multibeam Pulsar Survey (PMPS; Lorimer et al. 2006) which is significantly less sensitive than PALFA and therefore biased towards nearby sources. The increased sensitivity of PALFA not only allows higher DMs, and thus distances, to be probed, but allows discoveries of nearby pulsars to a lower luminosity. The MSPs discovered in PALFA will therefore provide valuable input to models of the Galactic MSP population – especially the population that is confined to the Galactic plane.

High-DM MSPs also provide unique probes into the properties of the interstellar medium (ISM). As pulsar signals propagate through the ISM, their signals are both dispersed (frequency-dependant delay), and scattered (multi-path propagation). These effects are time variable because of the pulsar’s proper motion and thus our changing line-of-sight through the ISM. Detailed dispersion and scattering measurements of signals from high-DM MSPs can be used to compare the observed effects to the predicted, thus improving our models of scattering and time-dependant DM variations. This is important for the detection of gravitational waves, as correcting the effects of DM variations and scattering can greatly increase the precision with which we time some MSPs (Keith et al. 2013).

PALFA has discovered 18 Galactic plane MSPs to date, including seven that have been published in previous works (Champion et al. 2008; Deneva et al. 2012; Crawford et al. 2012). These include: PSR J1950+2414, an eccentric MSP binary that may have formed via accretion induced collapse (Knipsel et al. in prep; Freire & Tauris 2014); and two MSPs for which Shapiro delay measurements were

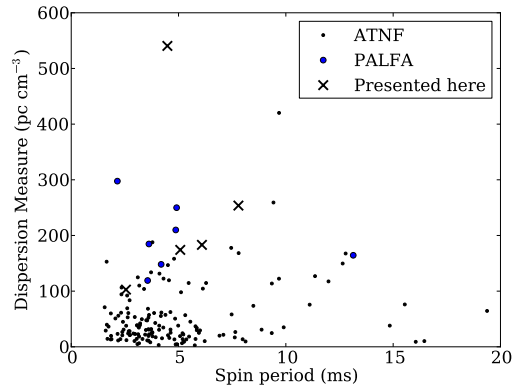


Figure 1. Period vs dispersion measure for all known Galactic MSPs (cf. Figure 5 of Crawford et al. 2012). PALFA provides a unique window at high DMs and fast spin periods. The PALFA pulsars are from Champion et al. (2008); Deneva et al. (2012); Crawford et al. (2012). The ‘ATNF’ MSPs are for all Galactic MSPs listed in the ATNF pulsar catalog (Manchester et al. 2005)^a.

made, PSR J1903+0327 (Champion et al. 2008) and PSR J1949+3106 (Deneva et al. 2012).

In this paper we present five PALFA MSP discoveries: PSRs J0557+1551, J1850+0244, J1902+0300, J1905+0453, and J1943+2210. The remaining six unpublished PALFA-discovered MSPs will be presented in forthcoming papers along with future discoveries. Section 2 describes the discoveries as well as the follow-up timing observations and analysis. In Section 3 we discuss the results of our timing analysis and explore the interesting properties of these newly discovered pulsars. In Section 4, we summarize our conclusions.

2. OBSERVATIONS & ANALYSIS

2.1. Discovery

The five MSPs presented here were discovered in PALFA survey observations taken between 2011 September and 2013 June. The PALFA survey currently uses the Mock spectrometers²⁰ as a backend for the 7-beam ALFA receiver at a central frequency of 1375 MHz. The Mock backend provides 322.617 MHz of bandwidth and a time resolution of $65.476 \mu\text{s}$ for each beam of ALFA. PALFA has survey regions towards both the inner and outer Galactic plane. The outer-galaxy pointings are provided by our commensal partners, the ALFA Zone-of-Avoidance Survey, who are mapping extragalactic neutral hydrogen emission behind the Galactic plane (Henning et al. 2010). A typical inner-galaxy survey pointing is 268 s and the outer-galaxy pointings are typically 180 s in length. Four of the five pulsars presented here were discovered using the above setup with the Mock backend in the inner galaxy. PSR J0557+1551 was discovered with the Mock backend in an outer-galaxy pointing. The discovery observation dates for each pulsar are listed in Table 1.

PALFA survey observations are processed by several pipelines. One of these is based on the PRESTO software package (Ransom et al. 2002)²¹ and is described in

¹⁹ <http://www.atnf.csiro.au/research/pulsar/psrcat/>

²⁰ <http://www.naic.edu/~astro/mock.shtml>

²¹ <http://www.cv.nrao.edu/~sransom/presto/>

Lazarus et al. (in prep). In brief, the PRESTO-based pipeline operates on raw data automatically downloaded from a PALFA-administered archive at the Cornell Center for Advanced Computing and is processed on Guilimin, a Compute Canada/Calcul Québec facility operated by McGill University. Some processing was also performed on dedicated computer clusters at the University of British Columbia and McGill University. Searches are performed both in the Fourier domain, for periodic sources, and in the time domain, for single pulses, using standard PRESTO tools. PALFA observations are also searched by the Einstein@Home pulsar search pipeline which uses distributed volunteer computing and is described in Allen et al. (2013). Lastly, a ‘quicklook’ pipeline (also PRESTO-based), which searches reduced-resolution data in near realtime at the telescope, is also employed. Four of the pulsars in this work were discovered using the full-resolution PRESTO-based pipeline and one, PSR J1943+2210, was discovered with the quicklook pipeline.

2.2. Timing Observations

Once confirmed as pulsars, we commenced timing observations of the five new MSPs in order to determine their rotational ephemerides. Timing observations began at the Lovell telescope at Jodrell Bank Observatory shortly after discovery and Arecibo observations began up to a year later.

Follow-up observations at Jodrell Bank used a dual-polarization cryogenic receiver on the 76-m Lovell telescope, having a system equivalent flux density of 25 Jy. Data were processed by a digital filterbank which covered the frequency band between 1350 MHz and 1700 MHz with channels of 0.5-MHz bandwidth. Observations were typically made with a total duration of 10 – 60 minutes, depending upon the discovery signal-to-noise ratio. Data were folded at the nominal topocentric period of the pulsar for subintegration times of 10 seconds. After “cleaning” of any radio-frequency interference (RFI) using a median zapping algorithm, followed by visual inspection and manual removal of any remaining RFI, the profiles were incoherently dedispersed at the nominal value of the pulsar DM. Initial pulsar parameters were established by conducting local searches in period and DM about the nominal discovery values and finally summed over frequency and time to produce integrated profiles.

The Arecibo observations were performed with the L-wide receiver which has a frequency range of 1150–1730 MHz and a system equivalent flux density of 3 Jy. The Puerto Rico Ultimate Pulsar Processing Instrument (PUPPI) backend was used to record the data. Initially, each pulsar was observed in incoherent search mode with PUPPI, where a full 800-MHz-wide spectrum in 2048 channels is read out every 40.96 μ s. This produces a high data volume, so each observation was post-processed by downsampling to 128 channels while correcting for delays due to dispersive effects from the interstellar medium within each channel before summing. Later observations were performed with PUPPI in coherent-dedispersion mode (hereafter referred to as coherent mode) where pulse profiles were folded in real-time and recorded in 10-s integrations with 512 frequency channels. Data from outside of the 1150–1750 MHz L-wide band were removed. Radio frequency interference

was excised with both automatic algorithms and manually using the PSRCHIVE (Hotan et al. 2004)²² tools `paz` and `psrzap`. Typically, each pulsar was observed for 10 min per observing session, except for PSR J0557+1551 which was observed for \sim 30 min–1 hour per session.

2.3. Timing Analysis

Initial timing solutions were obtained using solely Jodrell Bank observations. For the binary MSPs, orbital solutions were found by measuring the frequency of the pulsar in each observation and fitting a model of orbital Doppler shifts for a circular orbit. These orbital solutions were used as a starting point in the iterative timing procedure. Pulse times-of-arrival (TOAs) were obtained after matching with a standard template constructed from the Jodrell Bank observations and processed using standard pulsar timing techniques with PSRTIME and TEMPO²³.

The Arecibo observations were processed using standard PSRCHIVE tools. Using `pat`, TOAs for each of the early Arecibo observations were extracted by cross-correlating in the Fourier domain (Taylor 1992) the folded profile with a noise-free Gaussian template derived from the first Arecibo observation. TOA errors were derived using a Markov chain Monte Carlo method (FDM algorithm in `pat`). These TOAs were then fitted with timing solutions using TEMPO. Our timing analysis used the JPL DE405 solar-system ephemeris (Standish 1998) and the UTC(NIST) time standard.

In order to obtain the final timing solution presented here a high signal-to-noise template for each pulsar was constructed. To construct the templates, the Arecibo subbanded search mode observations were folded with the best ephemeris. A high signal-to-noise profile was then constructed by summing the profiles together, weighting by the signal-to-noise ratio of each observation. The summed profiles were subsequently smoothed using the PSRCHIVE tool `psrsmooth` to create a final template profile. For PSR J0557+1551, the procedure outlined above was used to construct a template profile, but using the coherent-mode data instead. Figure 2 shows the summed profiles and smoothed templates. The smoothed templates were used to extract TOAs that were used in the final TEMPO fit.

For nearly circular binary systems, there is a high correlation between the longitude of periastron, ω , and the epoch of periastron passage, T_0 , in timing models. Since the four binary pulsars presented here are nearly circular, we use the ELL1 orbital model (Lange et al. 2001) in TEMPO. It is parameterized with $\epsilon_1 = e \sin \omega$, $\epsilon_2 = e \cos \omega$, and $T_{asc} = T_0 - \omega P_b / 2\pi$, where e is the eccentricity, T_{asc} is the epoch of the ascending node, and P_b is the orbital period. This parameterization breaks the covariance but it is an approximation to first order in e and so is valid only when xe^2 is much smaller than the TOA precision. This is true for all the binary MSPs we are timing here.

The TOA uncertainties for each telescope and data-taking mode (Jodrell Bank, Arecibo incoherent-search mode, and Arecibo coherent mode) were increased by a scaling factor (EFAC) that yields a reduced χ^2 equal to unity. This results in more conservative estimates for the

²² <http://psrchive.sourceforge.net/>

²³ <http://tempo.sourceforge.net/>

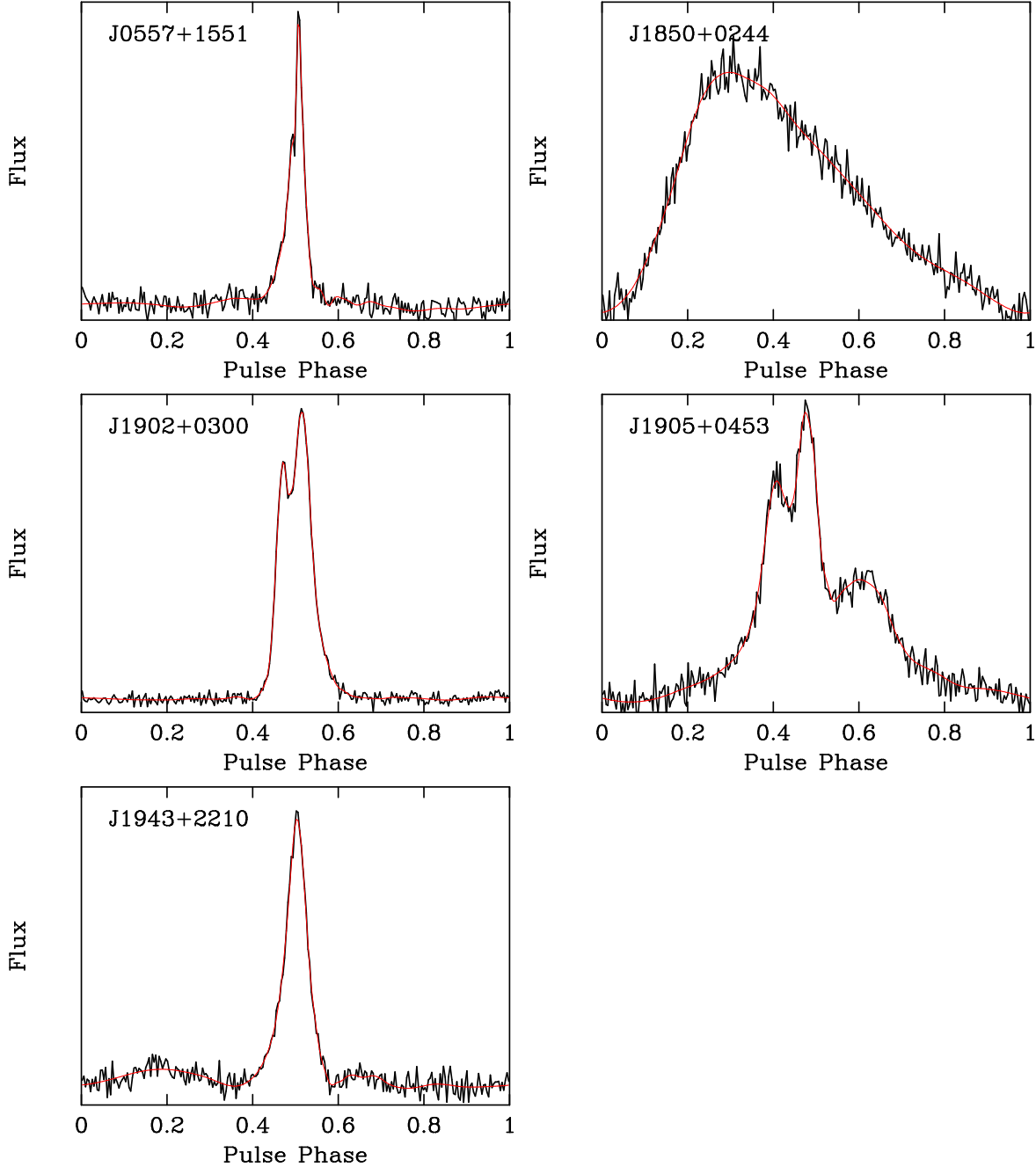


Figure 2. 1.4-GHz pulse profiles for the MSPs presented here. One full period is shown in 256 bins for each pulsar. The profiles were constructed by phase aligning and summing the Arecibo observations. The heavy black line shows the summed profiles and the light red line shows the profiles after smoothing was applied. The smoothed profiles were used as template for the generation of TOAs.

timing parameter uncertainties. This is standard practice in pulsar timing and it is well known that formal TOA uncertainties are often underestimated. These scaling factors (EFACs) are listed in Table 1 along with our best-fit timing solutions and derived parameters. The residuals are shown in Figure 3. The quoted uncertainties in 1 are 68% confidence limits as reported by TEMPO.

To make a refined measurement of the DM for each pulsar, we split the 600-MHz bandwidth of each PUPPI observation into six frequency bands and derived six TOAs from each observation for each 100-MHz band. We took our best-fit solution for each pulsar and held all param-

eters except for DM fixed. We then fit the TOAs using all frequency bands to measure a DM. DMs measured in this fashion are listed in Table 1.

We also fit for proper motions for PSRs J0557+1551, J1902+0300, and J1905+0453. We found that for all three sources the measured values were consistent with no proper motion in either right ascension or declination within 95.4% (2σ) confidence intervals. The upper limits on the total proper motion are shown in Table 1. The timing baselines for PSRs J1850+0244 and J1943+2210 were not long enough to break degeneracies with other parameters and place meaningful limits on the proper

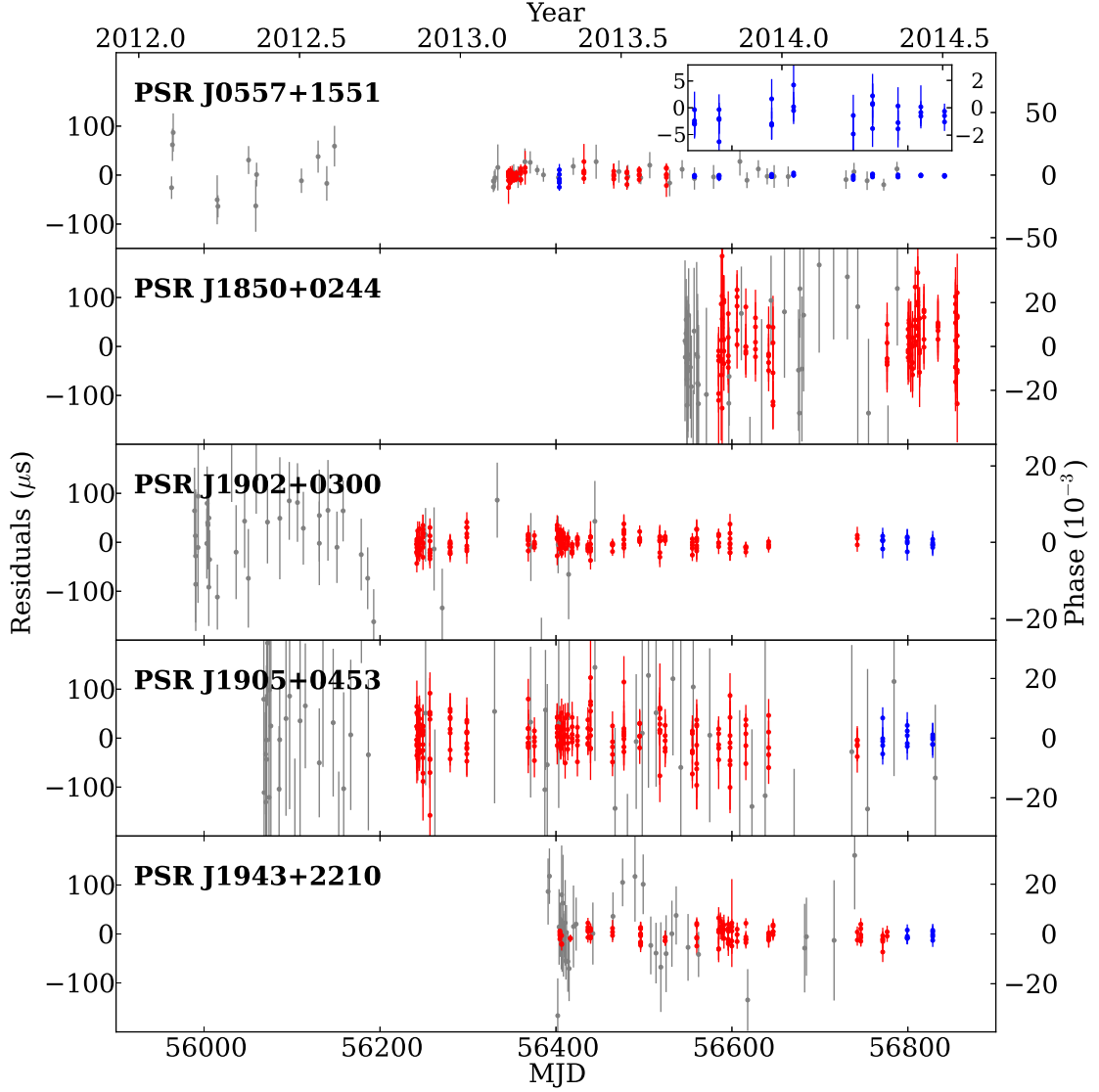


Figure 3. Timing residuals for the five MSPs. Gray points indicate Jodrell Bank TOAs, red points denote PUPPI search-mode TOAs and blue points represent PUPPI coherent-mode TOAs. The inset shows a zoom-in of the Arecibo coherent-mode observations for PSR J0557+1551. The x-axes of the inset are aligned with those of the main plot. Error bars are scaled so that the best-fit reduced χ^2 is equal to unity. The scaling factors along with rms values for the residuals are presented in Table 1.

motion.

2.4. Flux and Polarization Measurements

The Arecibo coherent-mode observations were flux- and polarization-calibrated using observations of a noise diode and of bright quasars (J1413+1509 and B1442+10) observed for the NANOGrav collaboration (Demorest et al. 2013). The calibrations were performed using the PSRCHIVE tool `pac` and the *SingleAxis* model, which assumes that the two polarization receivers are perfectly orthogonal. These calibrated observations provide a full set of Stokes parameters for each 10-s integrated pulse profile and so measurements of the flux and polarization characteristics are possible. Observations in this mode were made for four of the five pulsars, with

PSR J1850+0244 being the exception due to its more recent discovery. The set of calibrated coherent-mode observations were summed and Figure 4 shows the summed polarization profiles for each of the four pulsars.

In order to measure and correct for the effect of Faraday rotation on the polarization of the pulsars, rotation measures (RMs) were determined by summing the profiles in eight frequency sub-bands for all the calibrated coherent-mode observations. A set of trial RMs was tested by appropriately rotating Stokes U and Q for each frequency channel and then measuring the total linearly polarized flux, L . The RM and its uncertainty were then measured from the RM- L curve. Only PSR J0557+1551 provided a significant measurement

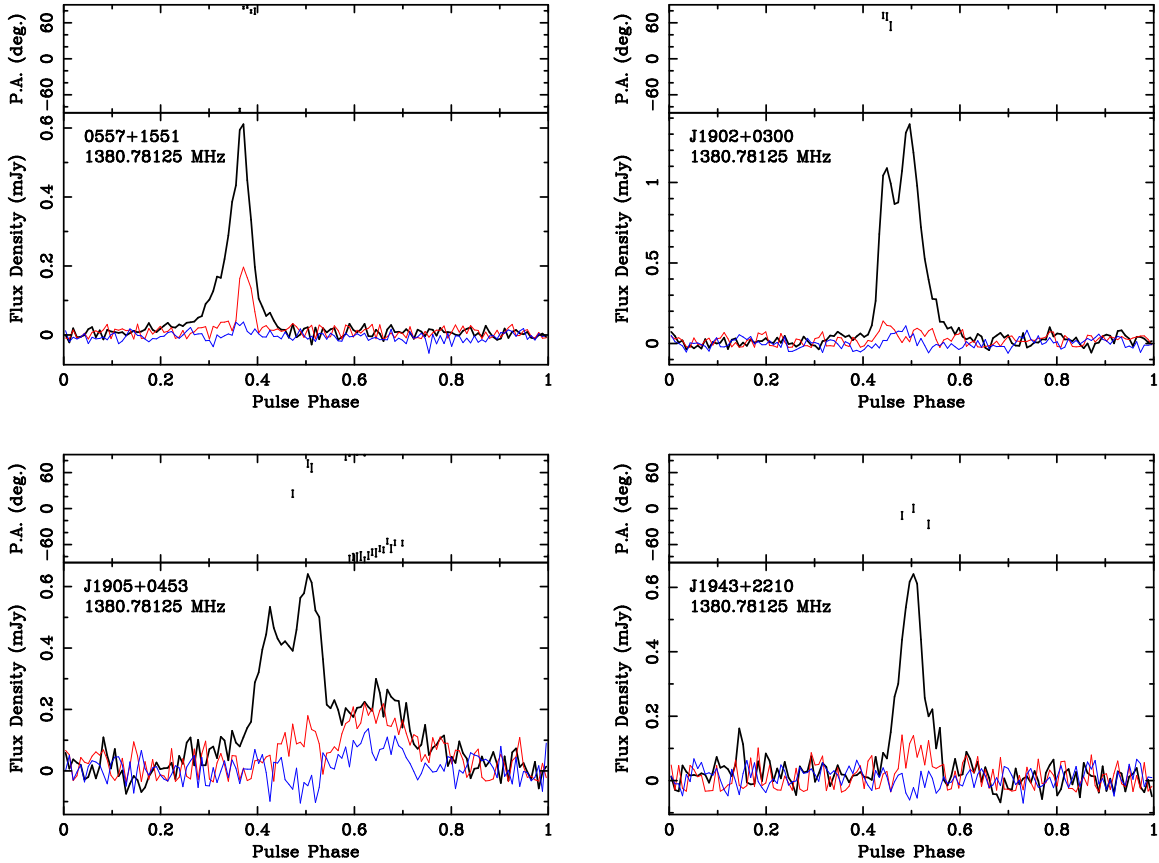


Figure 4. Polarization profiles for the four MSPs that had data taken with full Stokes parameters. In the bottom panel of each plot, the black, red, and blue lines show the total, linearly polarized, and circularly polarized flux, respectively. The top panels show the position angle of the linear polarization for profile bins with a linear polarization having a signal-to-noise greater than three. An RM could only be determined for PSR J0557+1551 and so its polarization has been corrected for Faraday rotation whereas the others have not.

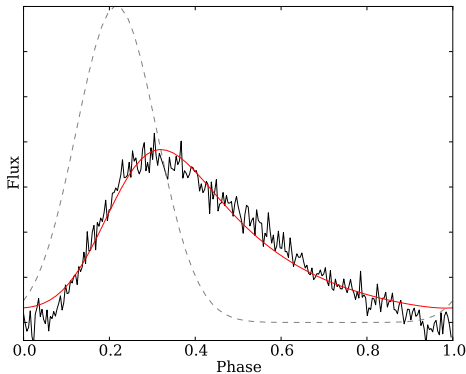


Figure 5. Pulse profile of PSR J1850+0244 (black line) fitted with a wrapped exponentially modified gaussian (red line). The unscattered gaussian, i.e. the underlying profile of the pulsar is represented by the dashed grey line. See text for parameters of the fit.

with $\text{RM} = 26 \pm 1 \text{ rad m}^{-2}$ where the uncertainty is statistical. This value may contain a contribution from ionospheric Faraday rotation. Han et al. (2006) find for RMs for 223 pulsars at 1.4 GHz that the ionospheric RM is typically between -1 and -5 rad m^{-2} . So we add in quadrature an uncertainty of $\pm 3 \text{ rad m}^{-2}$ to the measurement error to get $\text{RM} = 26 \pm 3 \text{ rad m}^{-2}$. The polarization profile of PSR J0557+1551 in Figure 4 has been corrected

for Faraday rotation using the measured RM value.

The calibrated observations were also used to measure the flux densities of the four pulsars. An off-pulse region was manually selected and its mean was subtracted from the calibrated profiles. For PSRs J1902+0300 and J1943+2210, the phase range excluding $\pm 15\%$ of pulse phase from the peak was used as the off-pulse region. For J0557+1551, due to its narrower pulse, $\pm 10\%$ from the peak was excluded. For J1905+0453, 30% of phase preceeding the peak and 40% following the peak was excluded. The mean flux density of the baseline-subtracted profile was then computed. Those values are presented in Table 1. Note that the quoted uncertainties are only statistical and do not take into account any uncertainties from the calibration procedure.

3. DISCUSSION

We have reported the discovery of five MSPs from the PALFA survey. We presented phase-coherent timing solutions of the five pulsars using observations from the Arecibo and Lovell telescopes. One of the pulsars was found to be isolated, and the rest are in nearly circular binaries. The DMs of the MSPs are high (see Figure 1), especially PSR J1850+0244 ($\text{DM} = 540 \text{ pc cm}^{-3}$), which is the highest DM MSP yet discovered. PALFA has to date discovered 18 MSPs. All but one, and all five presented in this work, have DMs greater than 100 pc cm^{-3} . This range is in the top 15% of non-PALFA Galactic

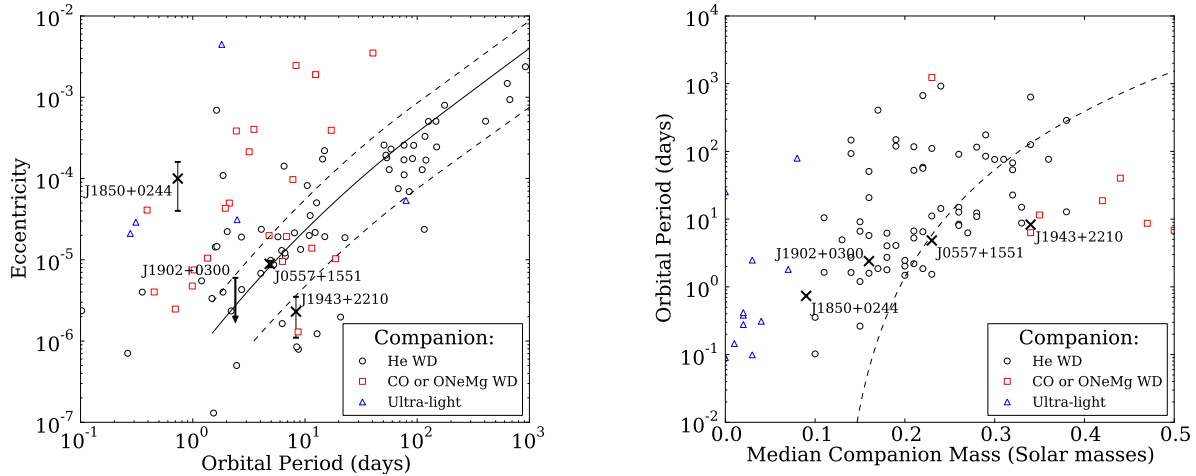


Figure 6. *Left:* Eccentricity as a function of orbital period for Galactic binary pulsars from the ATNF pulsar catalog. The solid line shows the relation from the HeWD-MSP binary formation model of Phinney & Kulkarni (1994) and the dotted lines show the 95% confidence intervals for that model. Crosses with error bars show the values and uncertainties at a 95% confidence level for the binary systems in this work. As the measured eccentricity for PSR J1902+0300 is consistent with zero it is shown as an upper limit. *Right:* Companion mass versus orbital period for Galactic field binary pulsars from the ATNF pulsar catalog. The dotted line shows the relation predicted by Tauris & Savonije (1999) for MSP-WD systems formed from LMXBs. Crosses show the four binary systems presented in this work. Other symbols represent the type of companion as tabulated in the ATNF pulsar catalog.

MSPs and the addition of the PALFA discovered MSPs represents a 70% increase in the number of MSPs with $DM > 100 \text{ pc cm}^{-3}$. Fourteen of the PALFA-discovered MSPs have DM/P ratios larger than $30 \text{ pc cm}^{-3} \text{ ms}^{-1}$, compared to 16 non-PALFA Galactic MSPs. PALFA discoveries have thus almost doubled the number of known Galactic MSPs with DM/P ratios larger than this value (Figure 1). Here we discuss some of the notable properties of each of the five MSPs.

3.1. PSR J0557+1551

PSR J0557+1551 is the most rapidly rotating of the five MSPs with a period of 2.55 ms. It is in a 4.9-day binary orbit and it has a DM of 103 pc cm^{-3} . Its DM implies a distance, estimated from the NE2001 model of Galactic free-electron content (Cordes & Lazio 2002), of 2.9 kpc. The minimum companion mass (i.e. the mass implied by the measured mass function assuming an orbital inclination angle of $i = 90^\circ$ and a pulsar mass of $1.4 M_\odot$) is $0.20 M_\odot$ and the median companion mass (i.e. $i = 60^\circ$) is $0.23 M_\odot$. Our timing solution has an rms residual of $4.9 \mu\text{s}$ and spans 2.4 years. PSR J0557+1551 is located in the Galactic anticenter and so is in a region with a relatively low density of known pulsars. Since its rms residuals and TOA errors are close to those in existing pulsar timing arrays (e.g. Demorest et al. 2013), along with the fact that it is located in an area where pulsar timing arrays presently have low sensitivity (e.g. Arzoumanian et al. 2014), it may be a good candidate for use in gravitational wave detection.

3.2. PSR J1850+0244

PSR J1850+0244 is the highest DM MSP yet discovered (540 pc cm^{-3}); its DM-derived distance is 10.4 kpc, the furthest for any known Galactic MSP. It has a spin period of 4.48 ms and is in a 0.74-day orbit with a companion with minimum and median masses of $0.07 M_\odot$ and $0.09 M_\odot$, respectively. The timing solution for this pulsar has an rms residual of $57 \mu\text{s}$ and spans 10 months.

The profile of PSR J1850+0244 shows a clear scattering tail. It also shows a slow rise implying that the underlying pre-scattered profile is quite broad. We fit the profile with a wrapped exponentially modified Gaussian, i.e. an underlying Gaussian profile convolved with an exponential decay, caused by the scattering, that is wrapped at the period of the pulsar. We show the pulse profile in Figure 5 along with the resulting best-fit exponentially modified Gaussian model. The best-fit exponential decay timescale was found to be $1.02 \pm 0.04 \text{ ms}$; this is close to the value predicted for scattering at 1.4 GHz by the NE2001 model of 1.3 ms. The best-fit width parameter of the underlying Gaussian is $\sigma = 0.41 \pm 0.02 \text{ ms}$ which corresponds to a width at 50% of the peak of $W_{50} = 0.97 \text{ ms}$ (a $\sim 20\%$ duty cycle). We caution that the exponentially-convolved Gaussian fitting function is only an approximation to the scattering of the actual pulse shape (Bhat et al. 2004), and that the above quoted uncertainties in the scattering time and intrinsic pulse width are solely statistical, and do not take into account the likely dominant systematic uncertainties from such an approximation.

3.3. PSR J1905+0453

PSR J1905+0453 is an isolated pulsar with a spin period of 6.09 ms, a DM of 183 pc cm^{-3} , and a DM-implied distance of 4.7 kpc. Its timing solution has an rms residual of $33 \mu\text{s}$ and spans 2.1 years.

PSR J1905+0453 has the second longest period out of all known isolated MSPs (PSR J1730–2304, with a spin period of 8.12 ms has the longest period among isolated MSPs; Lorimer et al. 1995). It also has the lowest \dot{E} out of any known isolated MSP ($1 \times 10^{33} \text{ erg s}^{-1}$). Isolated recycled pulsars are thought to originate from disruption due to a second supernova (Lorimer et al. 2004), ejection from a triple system (Freire et al. 2011), or ablation of the companion by the pulsar wind (Fruchter et al. 1990; Bailes et al. 2011). The short spin period requires a com-

panion lifetime that is much longer than that of stars massive enough to explode as supernovae. Ablation requires enough spin-down luminosity to power a pulsar wind that can disintegrate its companion. The question is then whether or not the low \dot{E} of PSR J1905+0453 would have been sufficiently large to power ablation earlier in its life as an MSP.

The \dot{P} , and thus \dot{E} , of PSR J1905+0453 will be biased by the acceleration in the Galactic plane. Using the formulae from Nice & Taylor (1995), we find that the motion of PSR J1905+0453 in the Galactic plane causes an effective \dot{P} of 1.3×10^{-21} and that the acceleration in the direction perpendicular to the plane is negligible. The corrected \dot{P} and \dot{E} are thus 4.0×10^{-21} and $7.0 \times 10^{32} \text{ erg s}^{-1}$.

The \dot{P} of PSR J1905+0453 could also be influenced by the Shklovskii effect whereby the space velocity relative to the observer causes an apparent contribution to \dot{P} . Since the proper motion measurement for PSR J1905+0453 is only an upper limit, the contribution from the Shklovskii effect cannot be calculated. However, if we assume that the observed \dot{P} is caused exclusively by the Shklovskii effect, it implies a transverse velocity of 200 km/s. This is a reasonable velocity; according to the ATNF pulsar catalog, $\sim 40\%$ of pulsars with measured proper motions have inferred transverse velocities equal or greater than 200 km/s. The true \dot{P} , and hence \dot{E} , of PSR J1905+0453 could therefore be much lower than the value in Table 1.

For now, let us assume that the contribution from the Shklovskii effect is minimal. The spin-down luminosity of PSR J1905+0453 was of course higher in the past. If we assume pure magnetic-dipole braking, a constant magnetic field, and that the MSP was recycled at most 14 Gyr ago (the age of the Universe), the fastest period and highest \dot{E} that PSR J1905+0453 could have had at formation would be 3.34 ms and $8 \times 10^{33} \text{ erg s}^{-1}$, respectively. This spin-down luminosity is comparable to those of several black widow pulsars, the least energetic of which have $\dot{E} \sim 1 \times 10^{34} \text{ erg s}^{-1}$ (Roberts 2013). Since black widow pulsars are thought to be in the process of ablating their companion, this suggests that it may have been possible for PSR J1905+0453 to have done so given its spin-down power if it originated in a binary similar to those of known black widow pulsars and the contribution of the Shklovskii effect to its measured \dot{E} is not dominant.

3.4. PSR J1902+0300

PSR J1902+0300 has a period of 7.80 ms, a DM of 254 pc cm^{-3} , and a NE2001 implied distance of 5.9 kpc. It is in a 2.4-day orbit and its companion has a minimum mass of $0.14 M_{\odot}$ and a median mass of $0.16 M_{\odot}$. Our timing solution has an rms residual of $14 \mu\text{s}$ and spans 2.3 years.

3.5. PSR J1943+2210

PSR J1943+2210 has a period of 8.31 ms, a DM of 174 pc cm^{-3} , and a NE2001 implied distance of 6.2 kpc. It is in a 8.3-day orbit with a minimum companion mass of $0.28 M_{\odot}$ and a medium mass of $0.34 M_{\odot}$. Its timing solution has an rms residual of $13 \mu\text{s}$ and spans 1.2 years.

3.6. Counterparts in other wavelengths

Because the pulsars presented here are quite faint and distant we would probably not expect counterparts in other wavelengths to be easily detected. The brightest white dwarfs have optical absolute magnitudes of ~ 10 (Carroll & Ostlie 2007). The closest of the five binary systems in this work, according to their DM-derived distances, is PSR J0557+1551 at 3 kpc. At this distance a $M_V = 10$ white dwarf would have an apparent magnitude of ~ 22 . This is quite faint and it is likely that the actual companion is fainter than this.

To see whether we expect to see gamma-ray counterparts for the MSPs, we can compare the spin-down energy incident at the Earth, \dot{E}/D^2 of the pulsars here with those of the *Fermi* detected MSPs. According to the ATNF pulsar catalog, most *Fermi*-detected MSPs have $\dot{E}/D^2 > 10^{33} \text{ erg s}^{-1} \text{ kpc}^{-2}$. Only PSR J0557+1551 has a \dot{E}/D^2 higher than this, and it is possible that a significant portion of the measured \dot{P} is due to the Shklovskii effect. Furthermore, the other four MSPs are located in the inner Galactic plane where the gamma-ray background is high.

Indeed, we find no coincident optical, infrared, X-ray or γ -ray sources in the SIMBAD²⁴ or HEASARC²⁵ databases or in the *Fermi* LAT 2-year Point Source Catalog (Nolan et al. 2012) for any of the MSPs reported here.

3.7. Nature of the Binary Companions

None of the four binaries presented here show any evidence for eclipses or matter in the system in their timing residuals, which suggests that none of the companions are likely close to filling their Roche lobes. Given the orbital separation and masses of the components of a binary system, the size of the Roche lobe of the companion can be calculated (Tauris & van den Heuvel 2006). If we assume a typical inclination of 60° and a pulsar mass of $1.4 M_{\odot}$, the sizes of the companion Roche lobes for all four binary systems can accommodate both white dwarfs and main sequence stars.

In Figure 6 we plot the binary parameters of the four binary MSPs presented here along with those from all Galactic-field binary MSPs, taken from the ATNF pulsar catalog. The plots of orbital period versus eccentricity and companion mass versus orbital period allow us to compare the binary parameters to the predicted relations from Phinney & Kulkarni (1994) and Tauris & Savonije (1999) for helium white-dwarf (HeWD)-MSP binaries that evolved through long-term, stable, mass transfer from a red giant progenitor onto a neutron star in a low-mass X-ray binary (LMXB).

The median companion masses implied by the mass functions of PSR J1902+0300 and PSR J0557+1551 are in the range expected for HeWD companions (Tauris et al. 2012). They also fall on the orbital period-eccentricity relation predicted by Phinney & Kulkarni (1994) and near the companion mass-orbital period relation predicted by Tauris & Savonije (1999). Thus, the likely nature of their companions are HeWDs.

²⁴ <http://simbad.u-strasbg.fr/simbad/>

²⁵ <http://heasarc.gsfc.nasa.gov/>

The other two binary systems fall slightly outside of the parameters expected for a system with a HeWD companion and so formation scenarios other than LMXB evolution into a HeWD may have occurred. PSR J1943+2210 has a companion mass that is higher than expected for a HeWD and falls outside of the relation from Phinney & Kulkarni (1994) with a lower than expected eccentricity. The high companion mass implies that its companion could be a carbon-oxygen white dwarf. It would therefore be considered an intermediate-mass binary pulsar (IMBP; Camilo 1996) a class of currently about 20 objects (Tauris et al. 2012).

PSR J1850+0244, on the other hand, has a lower mass than expected for a HeWD and a higher than predicted eccentricity. In the $M_c - P_b$ plot of Figure 6, it falls close to the systems classified as “Ultra-light”, many of which are considered black widows (Roberts 2013), raising the possibility that it has interacted with its companion through ablation and accretion processes, as the black-widow systems are thought to have done. Of course, the true companion mass of PSR J1850+0244 could be higher if the system has a low inclination. The relativistic MSP-HeWD binaries PSRs J0348+0432 and J1738+0333, which like PSR J1850+0244 have orbital periods less than a day and median companion masses $\sim 0.1 M_\odot$, have measured true companion masses determined from their post-Keplerian parameters and white dwarf spectroscopy. PSR J0348+0432 has a companion mass of $0.172 M_\odot$ and an inclination of 40° (Antoniadis et al. 2013). PSR J1738+0333 has a companion mass of $0.181 M_\odot$ and an inclination of 32° (Antoniadis et al. 2012). These companion masses are close to those predicted for HeWDs by Tauris & Savonije (1999). If we assume that PSR J1850+0244 has a HeWD companion with a mass of $0.19 M_\odot$ as predicted by Tauris & Savonije (1999), the inclination of the binary system would be 24° for a pulsar mass of $1.4 M_\odot$ and 30° for a pulsar mass of $2.0 M_\odot$. This is not an unreasonably fortuitous orientation and so it is plausible that PSR J1850+0244 has a low inclination and a standard HeWD companion.

3.8. Future prospects for mass measurements

Masses of the components in a MSP binary can be measured using the Shapiro delay effect (e.g. Ryba & Taylor 1991; Splaver et al. 2005; Demorest et al. 2010). The Shapiro delay is parameterized in timing models by the post-Keplerian parameters r and s . The Shapiro range, r , and shape, s , parameters are equal to the companion mass in units of light seconds and the sine of the inclination, respectively.

In the ELL1 model, when binary systems have measured $\epsilon_1 = e \sin \omega$ greater than zero and $\epsilon_2 = e \cos \omega$ consistent with zero, it may be the case that the eccentricity, e , is actually zero and the non-zero ϵ_1 is due to a Shapiro delay signal (Lange et al. 2001). For two of the four binary MSPs in this work, PSRs J0557+1551 and J1850+0244, $\epsilon_1 > 0$ and $\epsilon_2 = 0$. For these systems, given an assumed inclination, we can calculate the companion mass (i.e. Shapiro r) implied by the measured ϵ_1 assuming that the true eccentricity is consistent with zero (see Appendix A2 of Lange et al. 2001). If the implied companion masses are in a reasonable range given the measured mass functions, this would

give evidence that the measured ϵ_1 is due to Shapiro delay. For PSR J0557+1551, the lowest implied companion mass (i.e. at high inclination) is $\sim 2 M_\odot$ and for PSR J1850+0244 it is $\sim 2.5 M_\odot$. Since the measured mass functions for these two MSPs would require unreasonably high pulsar masses in order for their companions to be so heavy, this implies that the measured values of ϵ_1 for PSRs J0557+1551 and J1850+0244 are not dominated by Shapiro delay signals.

In order to test for a Shapiro delay signal in each of the binary pulsars, a timing model was fit using the TEMPO DD model (Damour & Deruelle 1985, 1986) which includes post-Keplerian parameters in the timing model. We fit the TOAs using TEMPO with the best-fit parameters listed in Table 1 with the addition of a test M_c and $\cos i$. We searched a grid of M_c and $\cos i$ ranging from $0.0 \leq M_c \leq 1.0$ and $0.0 \leq \cos i \leq 1.0$. For all but PSR J0557+1551, all points in the grid provided acceptable fits at greater than a 95.4% level and so no limits could be placed. For PSR J0557+1551, the left panel of Figure 7 shows the upper-limit contours placed on M_2 and $\cos i$. It is clear that a small portion of reasonable binary system parameters are inconsistent with the data at a 1σ confidence level, namely at high inclination and high pulsar mass.

These current limits are not very constraining, but future observations may yield interesting results. To investigate this, we constructed a simulated set of TOAs with uncertainties and rms residuals of approximately $1 \mu s$. The simulated timing campaign spanned a year with a one month cadence and included ten 2.5-h observations that each occurred at one of the ten conjunctions of the system that will be visible at Arecibo in that time span. The right panel of Figure 7 shows the limits that could be placed with such a campaign given a pulsar mass of $1.4 M_\odot$ and an inclination of 80° which imply a companion mass of $0.20 M_\odot$. Note that if PSR J0557+1551 has a more favorable binary configuration (i.e. higher component masses or inclination) or if the timing precision could be improved to better than $1 \mu s$ then more stringent measurements could be made with a campaign similar to that simulated.

4. CONCLUSIONS

The search for MSPs is heavily motivated by the unique and exciting studies that are enabled by finding more systems that provide laboratories for such science. PALFA provides a unique window on the MSP population, discovering more distant and fainter MSPs than any other past or current survey. We have presented here the discovery and follow-up timing of five MSPs discovered in the PALFA survey as well as discussed their interesting properties. One MSP, PSR J1905+0453 is isolated and has the lowest spin-down luminosity yet measured for an isolated MSP. Three of the binary MSPs likely have HeWD companions and one, PSR J1943+2210, may have a carbon-oxygen WD companion. At least one of the five, PSR J0557+1551, has the potential to allow mass measurements and may be useful in pulsar timing arrays. PSR J1850+0244 is the highest DM MSP yet discovered with a DM of 540. Further discoveries in the ongoing PALFA survey will expand our knowledge of the MSP population deep into the Galactic plane as well as help constrain fundamental physics and astrophysics.

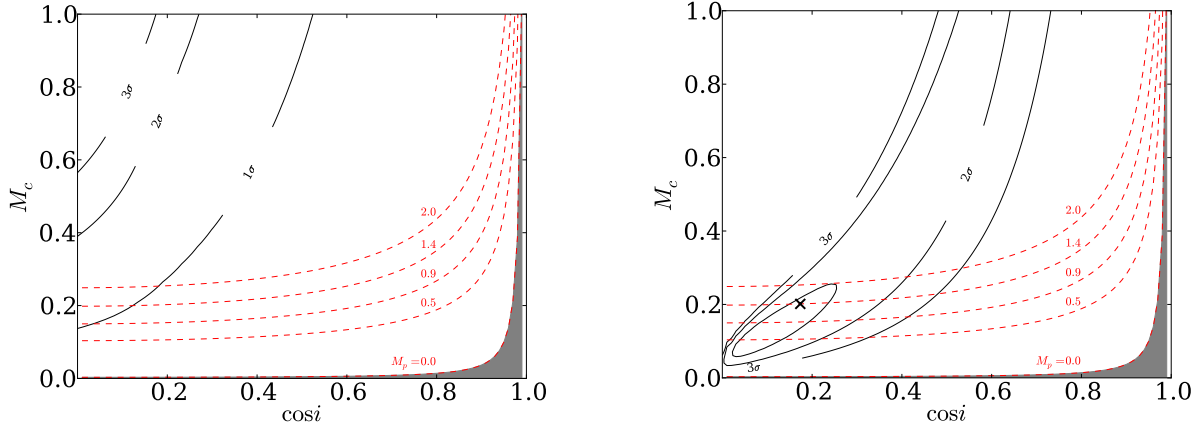


Figure 7. Maps of companion-mass and inclination angle for PSR J0557+1551. The left plot shows binary configurations allowed by current timing data and the right shows configurations for a simulated data set with $M_p = 1.35 M_\odot$ and $i = 80^\circ$ (see text). The black cross denotes the simulated binary configuration. The black contours enclose 68.3% (1σ), 95.4% (2σ), and 99.7% (3σ) of allowed configurations. The red dashed lines denote the pulsar mass for the configuration.

We thank the anonymous referee for their constructive comments. The Arecibo Observatory is operated by SRI International under a cooperative agreement with the National Science Foundation (AST-1100968), and in alliance with Ana G. Méndez-Universidad Metropolitana, and the Universities Space Research Association. P.S. acknowledges support from an NSERC Alexander Graham Bell Canada Graduate Scholarship. V.M.K. acknowledges support from an NSERC Discovery Grant and Accelerator Supplement, the FQRNT Centre de Recherche en Astrophysique du Québec, an R. Howard Webster Foundation Fellowship from the Canadian Institute for Advanced Research (CIFAR), the Canada Research Chairs Program and the Lorne Trottier Chair in Astrophysics and Cosmology. J.W.T.H. acknowledges funding from an NWO Vidi fellowship and ERC Starting Grant “DRAGNET” (337062). P.C.C.F. and L.G.S. gratefully acknowledge financial support by the European Research Council for the ERC Starting Grant BEACON under contract no. 279702. P.L. acknowledges the support of IMPRS Bonn/Cologne and FQRNT B2. Work at Cornell University was supported in part by the National Science Foundation (PHYS-PHY1104617). Pulsar research at UBC is supported by an NSERC Discovery Grant and Discovery Accelerator Supplement, and by the Canadian Institute for Advanced Research. Computations were made on the supercomputer Guilimin from McGill University, managed by Calcul Québec and Compute Canada. The operation of this supercomputer is funded by the Canada Foundation for Innovation (CFI), NanoQuébec, RMGA and the Fonds de recherche du Québec - Nature et technologies (FRQ-NT).

REFERENCES

- Allen, B., Knispel, B., Cordes, J. M., et al. 2013, *ApJ*, 773, 91
 Alpar, M. A., Cheng, A. F., Ruderman, M. A., & Shaham, J. 1982, *Nature*, 300, 728
 Antoniadis, J., van Kerkwijk, M. H., Koester, D., et al. 2012, *MNRAS*, 423, 3316
 Antoniadis, J., Freire, P. C. C., Wex, N., et al. 2013, *Science*, 340, 448
 Archibald, A. M., Stairs, I. H., Ransom, S. M., et al. 2009, *Science*, 324, 1411
 Arzoumanian, Z., Brazier, A., Burke-Spolaor, S., et al. 2014, *ApJ*, submitted; arXiv:1404.1267
 Backer, D. C., Kulkarni, S. R., Heiles, C., Davis, M. M., & Goss, W. M. 1982, *Nature*, 300, 615
 Bailes, M., Bates, S. D., Bhalariao, V., et al. 2011, *Science*, 333, 1717
 Bailyn, C. D., & Grindlay, J. E. 1990, *ApJ*, 353, 159
 Bednarek, I., Haensel, P., Zdunik, J. L., Bejger, M., & Mańka, R. 2012, *A&A*, 543, A157
 Bhat, N. D. R., Cordes, J. M., Camilo, F., Nice, D. J., & Lorimer, D. R. 2004, *ApJ*, 605, 759
 Camilo, F. 1996, in *Pulsars: Problems and Progress*, IAU Colloquium 160, ed. S. Johnston, M. A. Walker, & M. Bailes (San Francisco: Astronomical Society of the Pacific), 539
 Carroll, B. W., & Ostlie, D. A. 2007, *An introduction to modern astrophysics* (San Francisco, CA : Addison-Wesley)
 Champion, D. J., Ransom, S. M., Lazarus, P., et al. 2008, *Science*, 320, 1309
 Cordes, J. M., & Lazio, T. J. W. 2002, *astro-ph/0207156*
 Cordes, J. M., Freire, P. C. C., Lorimer, D. R., et al. 2006, *ApJ*, 637, 446
 Crawford, F., Stovall, K., Lyne, A. G., et al. 2012, *ApJ*, 757, 90
 Damour, T., & Deruelle, N. 1985, *Ann. Inst. H. Poincaré (Physique Théorique)*, 43, 107
 —. 1986, *Ann. Inst. H. Poincaré (Physique Théorique)*, 44, 263
 Demorest, P. B., Pennucci, T., Ransom, S. M., Roberts, M. S. E., & Hessels, J. W. T. 2010, *Nature*, 467, 1081
 Demorest, P. B., Ferdman, R. D., Gonzalez, M. E., et al. 2013, *ApJ*, 762, 94
 Deneva, J. S., Freire, P. C. C., Cordes, J. M., et al. 2012, *ApJ*, 757, 89
 Foster, R. S., & Backer, D. C. 1990, *ApJ*, 361, 300
 Freire, P. C. C., & Tauris, T. M. 2014, *MNRAS*, 438, L86
 Freire, P. C. C., Bassa, C. G., Wex, N., et al. 2011, *MNRAS*, 412, 2763
 Freire, P. C. C., Wex, N., Esposito-Farèse, G., et al. 2012, *MNRAS*, 423, 3328
 Fruchter, A. S., Berman, G., Bower, G., et al. 1990, *ApJ*, 351, 642
 Gonzalez, M. E., Stairs, I. H., Ferdman, R. D., et al. 2011, *ApJ*, 743, 102
 Han, J. L., Manchester, R. N., Lyne, A. G., Qiao, G. J., & van Straten, W. 2006, *ApJ*, 642, 868
 Henning, P. A., Springob, C. M., Minchin, R. F., et al. 2010, *AJ*, 139, 2130
 Hotan, A. W., van Straten, W., & Manchester, R. N. 2004, *Proc. Astr. Soc. Aust.*, 21, 302
 Johnston, H. M., & Kulkarni, S. R. 1991, *ApJ*, 368, 504
 Keith, M. J., Coles, W., Shannon, R. M., et al. 2013, *MNRAS*, 429, 2161
 Lange, C., Camilo, F., Wex, N., et al. 2001, *MNRAS*, 326, 274
 Lattimer, J. M., & Prakash, M. 2010, *ArXiv e-prints*
 Lazarus, P. 2013, in *IAU Symposium, Vol. 291, Neutron Stars and Pulsars: Challenges and Opportunities after 80 years*, ed. J. van Leeuwen, 35–40
 Levinson, A., & Eichler, D. 1991, *ApJ*, 379, 359
 Lorimer, D. R., Nicastro, L., Lyne, A. G., et al. 1995, *ApJ*, 439, 933
 Lorimer, D. R., McLaughlin, M. A., Arzoumanian, Z., et al. 2004, *MNRAS*, 347, L21

- Lorimer, D. R., Faulkner, A. J., Lyne, A. G., et al. 2006, *MNRAS*, 372, 777
- Manchester, R. N., Hobbs, G. B., Teoh, A., & Hobbs, M. 2005, *AJ*, 129, 1993
- Nice, D. J., & Taylor, J. H. 1995, *ApJ*, 441, 429
- Nolan, P. L., Abdo, A. A., Ackermann, M., et al. 2012, *ApJS*, 199, 31
- Papitto, A., Ferrigno, C., Bozzo, E., et al. 2013, *Nature*, 501, 517
- Phinney, E. S., & Kulkarni, S. R. 1994, *Ann. Rev. Astr. Ap.*, 32, 591
- Portegies Zwart, S., van den Heuvel, E. P. J., van Leeuwen, J., & Nelemans, G. 2011, *ApJ*, 734, 55
- Radhakrishnan, V., & Srinivasan, G. 1982, *Curr. Sci.*, 51, 1096
- Ransom, S. M., Eikenberry, S. S., & Middleditch, J. 2002, *AJ*, 124, 1788
- Ransom, S. M., Stairs, I. H., Archibald, A. M., et al. 2014, *Nature*, 505, 520
- Roberts, M. S. E. 2013, in *IAU Symposium*, Vol. 291, IAU Symposium, ed. J. van Leeuwen, 127–132
- Ryba, M. F., & Taylor, J. H. 1991, *ApJ*, 371, 739
- Shannon, R. M., Ravi, V., Coles, W. A., et al. 2013, *Science*, 342, 334
- Splaver, E. M., Nice, D. J., Stairs, I. H., Lommen, A. N., & Backer, D. C. 2005, *ApJ*, 620, 405
- Standish, E. M. 1998, *JPL Planetary and Lunar Ephemerides*, DE405/LE405, Memo IOM 312.F-98-048 (Pasadena: JPL), <http://ssd.jpl.nasa.gov/iau-comm4/de405iom/de405iom.pdf>
- Stovall, K., Lorimer, D. R., & Lynch, R. S. 2013, *Classical and Quantum Gravity*, 30, 224003
- Tauris, T. M., Langer, N., & Kramer, M. 2012, *MNRAS*, 425, 1601
- Tauris, T. M., & Savonije, G. J. 1999, *A&A*, 350, 928
- Tauris, T. M., & van den Heuvel, E. P. J. 2006, in *Compact stellar X-ray sources*, ed. W. H. G. Lewin & M. van der Klis (UK: Cambridge University Press), 623
- Taylor, J. H. 1992, *Phil. Trans. Roy. Soc. A*, 341, 117
- van Haasteren, R., Levin, Y., Janssen, G. H., et al. 2011, *MNRAS*, 414, 3117
- Yardley, D. R. B., Coles, W. A., Hobbs, G. B., et al. 2011, *MNRAS*, 414, 1777

Table 1
Timing Parameters for five MSPs

PSR J	0557+1551	1850+0244	1902+0300	1905+0453	1943+2210
Measured Parameters					
Right ascension (J2000)	05 : 57 : 31.44918(9)	18 : 50 : 41.683(1)	19 : 01 : 59.6168(1)	19 : 04 : 59.3848(2)	19 : 43 : 16.4910(1)
Declination (J2000)	15 : 50 : 06.046(8)	02 : 42 : 57.44(3)	03 : 00 : 23.324(5)	04 : 51 : 54.953(8)	22 : 10 : 23.151(2)
Total proper motion, μ_T (mas yr ⁻¹) ^a	< 80	-	< 77	< 96	-
Spin frequency, ν (s ⁻¹)	391.18012787837(8)	223.221059721(3)	128.25813729784(5)	164.1397912192(1)	196.6887956594(2)
Frequency derivative, $\dot{\nu}$ (s ⁻²)	$-1.125(3) \times 10^{-15}$	$-8.1(2) \times 10^{-15}$	$-7.52(2) \times 10^{-16}$	$-1.54(6) \times 10^{-16}$	$-3.4(1) \times 10^{-16}$
Dispersion measure, DM (pc cm ⁻³)	102.5723(5)	540.068(9)	253.887(2)	182.705(4)	174.089(3)
Orbital period, P_b (d)	4.846550440(4)	0.73543015(1)	2.399218509(6)	-	8.31148080(2)
Projected semimajor axis, $x = a \sin i/c$ (s)	4.0544597(8)	0.452355(9)	1.842553(1)	-	8.064088(2)
Time of ascending node, T_{asc} (MJD)	56349.2459263(2)	56468.179498(6)	55989.555577(1)	-	56392.7364900(7)
$e_1 = e \sin \omega$	$9.3(4) \times 10^{-6}$	$9(3) \times 10^{-5}$	$3(2) \times 10^{-6}$	-	$2.5(8) \times 10^{-6}$
$e_2 = e \cos \omega$	$-9(60) \times 10^{-8}$	$-4(40) \times 10^{-6}$	$4(10) \times 10^{-7}$	-	$-1.4(4) \times 10^{-6}$
Derived Parameters					
Galactic longitude, l (degrees)	192.68	35.26	36.81	38.81	58.44
Galactic latitude, b (degrees)	-4.31	1.40	-0.97	-0.79	-0.73
Period, P (ms)	2.5563670767830(5)	4.47986404710(6)	7.796776259723(3)	6.092367929629(5)	5.084173689952(5)
Period derivative, \dot{P}	$7.35(2) \times 10^{-21}$	$1.62(4) \times 10^{-19}$	$4.57(1) \times 10^{-20}$	$5.7(2) \times 10^{-21}$	$8.7(3) \times 10^{-21}$
Eccentricity, e	$9.3(4) \times 10^{-6}$	$9(3) \times 10^{-5}$	$3(2) \times 10^{-6}$	-	$2.9(7) \times 10^{-6}$
Longitude of periastron, ω (deg)	91(4)	90(20)	80(30)	-	$120(10) \times 10^2$
Time of periastron passage, T_0 (MJD)	56350.47(5)	56468.37(5)	55990.1(2)	-	56395.5(2)
Mass function (M_\odot)	$3.046605(2) \times 10^{-3}$	$1.8375(1) \times 10^{-4}$	$1.166818(2) \times 10^{-3}$	-	$8.150639(6) \times 10^{-3}$
Minimum companion mass (M_\odot) ^b	0.20	0.07	0.14	-	0.28
Median companion mass (M_\odot) ^c	0.23	0.09	0.16	-	0.34
Surface dipolar magnetic field, B (G)	$1.388(2) \times 10^8$	$8.6(1) \times 10^8$	$6.040(8) \times 10^8$	$1.89(3) \times 10^8$	$2.13(3) \times 10^8$
Spin-down luminosity, \dot{E} (erg s ⁻¹)	$1.738(5) \times 10^{34}$	$7.1(2) \times 10^{34}$	$3.81(1) \times 10^{33}$	$1.00(4) \times 10^{33}$	$2.61(8) \times 10^{33}$
Characteristic age, τ_c (yr)	$5.51(2) \times 10^9$	$4.4(1) \times 10^8$	$2.705(7) \times 10^9$	$1.69(6) \times 10^{10}$	$9.3(3) \times 10^9$
DM distance, D (kpc) ^d	2.9	10.4	5.9	4.7	6.2
Transverse velocity, V_T (km s ⁻¹) ^a	< 1100	-	< 2100	< 2100	-
Observation Parameters					
1400 MHz mean flux density, S_{1400} (mJy)	0.050(6)	-	0.113(4)	0.117(9)	0.04(1)
1400 MHz mean radio luminosity, L_{1400} (mJy kpc ²) ^e	~ 0.4	-	~ 3.9	~ 2.6	~ 1.5
Discovery observation date (MJD)	55907	56466	55863	55817	56389
Timing epoch (MJD)	56346.00	56554.29	56242.00	56242.00	56404.00
Start epoch (MJD)	55963.08	56546.71	55989.20	56067.92	56391.07
Finish epoch (MJD)	56841.65	56856.14	56828.22	56831.16	56828.25
Number of TOAs	162	160	270	278	147
Typical Integration time per Arecibo TOA (min)	10	2	2	2	2
Typical TOA uncertainty (μ s) (Jodrell/AO-search/AO-fold)	23/7/3	130/50/-	80/15/15	160/30/25	60/10/10
TOA error scale factor, EFAC (Jodrell/AO-search/AO-fold)	1.58/1.95/1.67	1.67/1.13/-	1.19/1.06/1.07	2.34/1.01/0.98	2.19/0.91/0.89
rms post-fit residuals (μ s)	4.87	57.12	13.92	32.92	13.31

Note. — Numbers in parentheses are TEMPO reported 1σ uncertainties.

^a 95.4% (2σ) upper limits.

^b Assuming a pulsar mass of $1.4 M_\odot$ and an inclination of 90° .

^c Assuming a pulsar mass of $1.4 M_\odot$ and an inclination of 60° .

^d As implied by the Cordes & Lazio (2002) NE2001 DM-distance model.

^e $L_{1400} = S_{1400} D^2$.